2001

Size scaling relationships in the active fault networks of Japan and their correlation with Gutenberg-Richter b values

Ali Osman Öncel

Thomas H. Wilson

Osamu Nishizawa

JOURNAL OF GEOPHYSICAL RESEARCH, VOL. 106, NO. B10, PAGES 21,827–21,841, OCTOBER 10, 2001

Size scaling relationships in the active fault networks of Japan and their correlation with Gutenberg-Richter *b* values

Ali Osman Öncel
Department of Geophysical Engineering, Istanbul University, Istanbul,Turkey

Thomas H. Wilson
Department of Geology and Geography, West Virginia University, Morgantown, West Virginia

Osamu Nishizawa
Geological Survey of Japan, Tsukuba, Japan

Abstract. Fractal properties of active fault systems in Japan are evaluated and compared to Gutenberg-Richter *b* values. Properties of the active fault network and seismicity were evaluated at 20 km intervals along three lines oriented along the length of Honshu, the main island of Japan. Fractal dimensions for the active fault network are calculated using the box counting method. The box curves often reveal the presence of an abrupt transition in slope at ~8 km scales. This transition separates linear regions in the box curves that span box sizes of 17.5 to 8.5 km and 7.75 to 2 km. Power law coefficients were computed for the 17.5 to 8.5 km (D_L) and 7.75 to 2 km (D_S) range of box sizes from overlapping 70x70 km regions of the active fault complex. The maximum likelihood method is used to estimate *b* value from earthquakes occurring in the seismogenic zone (upper 20 km). The correlation between *D* and *b* value are found to vary considerably throughout Japan. In general, *D* and *b* are negatively correlated, which suggests that increased complexity in the active fault network accommodates rupture along fault planes of relatively larger surface area. Areas of significant positive correlation are also observed in Japan. The positive correlations arise through joint increases in *b* and *D*. In such areas the probability of large magnitude earthquakes decreases in response to increased fragmentation of the active fault network and increased possibility that stress release will take place along faults of smaller surface area. Negative correlations between *b* and *D* generally occur when increases in *D* are paralleled by decreases in *b*. Negative correlation areas bound the intensely faulted region of central Japan. An area of negative correlation also occurs in the intensely faulted high *D* area of central Japan where continued increases in *D* are paralleled by decreases in *b*. In general, these observations suggest that as fault complexity increases (as measured by *D*), interconnected planes of larger and larger surface area will accommodate strain release. However, with continued rise in fault complexity, strain release begins to occur on smaller fragments resulting in higher *b* and lower-magnitude seismicity. The analysis may provide insights into the relationship between seismicity associated with large-scale faults populations and earthquake hazard assessment.

1. Introduction

In this paper, we examine possible relationships between the distribution of active faults and recent seismicity along the Japan Island Arc. The majority of seismicity and faulting in the Japanese Islands appears to be related to the continuing movement of two arc systems (the northeast and southwest Japan systems) toward Eurasia (Figure 1). The Japanese Islands are divided geologically into two different tectonic regimes at about 138°E roughly separating SW and NW Japan. This line roughly falls along the Itoigawa-Shizuoka Tectonic Line, which serves as the western boundary of the Fossa Magna region and eastern boundary of the Japan Alps. Seismicity in Japan is also categorized as Intraplate and interplate depending upon their tectonic origins. Intraplate events are shallow events that occur on land while the inter-plate events occur along major subduction zones such as those between the Philippine Pacific Sea plates along the Izu-Ogasawara Arc or along the Pacific and North American plates in northeast Japan. Earthquake recurrence for intraplate events is much longer than interplate events [*Shimazaki*, 1978].

Seismotectonics of Japan are controlled in general by horizontal shortening. Compressional stress is oriented roughly E-W but can be quite variable. For example, in the Izu Peninsula area tectonic stress has a more northerly orientation in response to the collision of the Izu-Ogasawara Arc with central Japan in that area. The characteristics of faulting along the Japan Island Arc are very complex and have

Paper number 2000JB900408.
0148-0227/01/2000JB900408$09.00

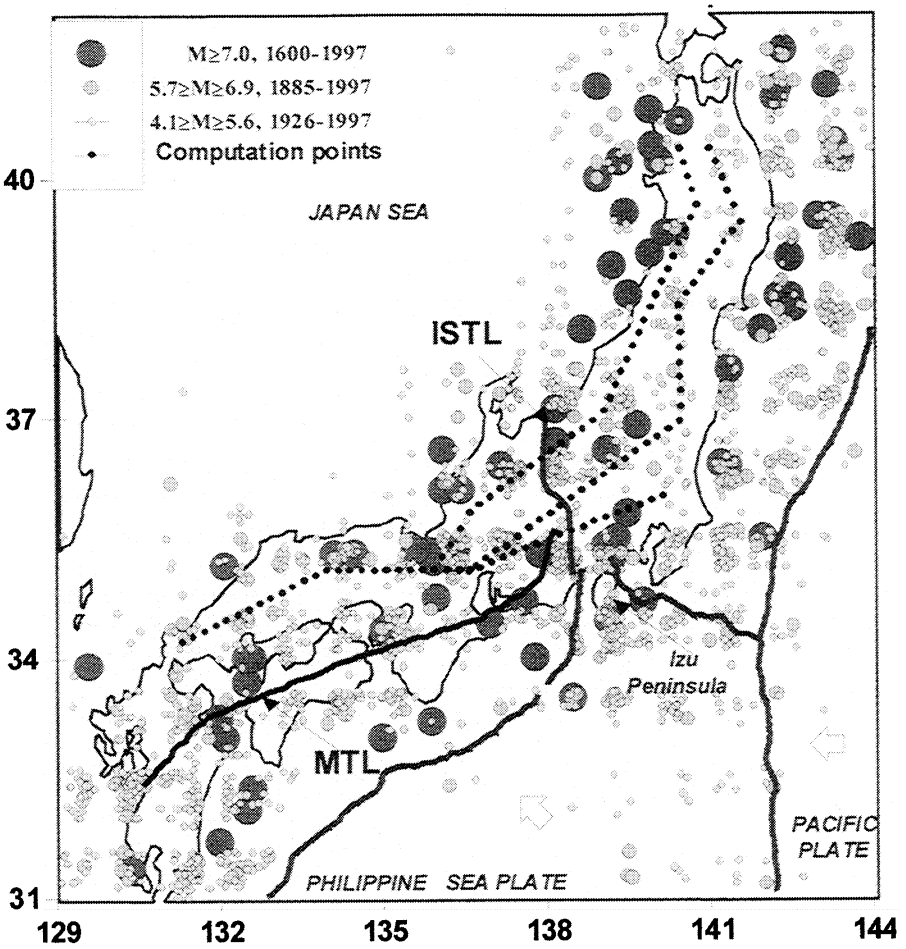

Figure 1. Shallow seismicity data (h<40 km) on land covering the period of time from 1600 to 1997. ISTL, Itoigawa-Shizuoka Tectonic Line; Median Tectonic Line.

been divided geographically into several subfault systems. These include the main part of Hokkaido, the inner and outer belts of Japan, continental slopes of the Pacific coast of NE Japan, northern tip of Izu-Ogasawara Arc, western Fossa Magna belt, eastern and western parts of Inner belt of SW Japan, Median Tectonic Line belt, outer belt of SW Japan, continental slopes of the Pacific coast of SW Japan, the Ryuku Arc, and Okinawa Trough [*Research Group for Active Faults of Japan*, 1995].

Analysis of active fault and seismicity data was conducted along lines that are oriented along the length of Honshu, the main island of Japan. Active fault patterns were analyzed using the box counting method to compute size-scaling properties of the active fault network. Computations of fractal dimensions were made of 70 kmx70 km regions spaced at 20 km intervals along each line. Seismicity along these lines was characterized using the Gutenberg-Richter b value. This is one of the most widely used statistical descriptions of seismicity and is obtained from the frequency-magnitude relationship for earthquakes:

$$\log N = a - b\,m, \qquad (1)$$

where N is the number of events with magnitude greater than m, and a and b are constants. The Gutenberg-Richter relationship was shown by *Aki* [1981] to be the equivalent of a fractal distribution [*Turcotte*, 1997]. Specifically, it can be shown that the b value is proportional to the fractal dimension in a power law relationship between the frequency of earthquake occurrence N and the area of fault rupture (A) such that

$$N = \beta A^{-b} \qquad (2)$$

where β is a constant of proportionality [see *Turcotte*, 1997]. Since $A \propto r^2$, where r is a characteristic linear dimension of the fault surface, equation (2) implies that $D = -2b$. This relationship has provided the basis for several studies including the present one. As *Turcotte* [1997] notes, the relationship implies one of two end-member relationships: either there is a fractal distribution of faults, each having its own characteristic earthquake, or there is a fractal distribution of earthquakes along any given fault. We test the idea on a regional scale that the fractal distribution of earthquake frequency implied by the Gutenberg-Richter relationship is associated with a fractal distribution of faults.

In summary, seismicity can be related to the characteristic linear dimension of the active fault networks through a fractal relationship [*Aki*, 1981]. The main purpose of this paper is to evaluate whether such a relationship between seismicity and active faulting exists for the Japan Island Arc. Further, if a relationship exists between these variables, how might such a relationship be pertinent to seismic hazard assessment?

2. Previous Studies

Previous studies of the active faults in Japan by *Hirata* [1989a] and *Matsumoto et al.* [1992] suggest that the active fault networks are fractal. Hirata's analysis covered most of Japan and was conducted on 1° longitude by 40 arc min latitude areas, roughly 90 by 74 km in size, using active fault sheet maps of Japan published by the *Research Group for Active Faults of Japan* [1980]. *Matsumoto et al.* [1992] analyzed narrow strip-like regions along the Median Tectonic Line and the Izu Peninsula using data from the *Research Group for Active Faults of Japan* [1980] and also the *Research Group for Active Tectonic Structures in Kyushu* [1989]. To estimate the fractal dimensions of active fault distributions, *Matsumoto et al.* [1992] employed a method different from Hirata's method. Hirata used a box counting method [e.g., *Turcotte* 1989, 1992], while *Matsumoto et al.* [1992] used the method of *Okubo and Aki* [1987], which is based on the relationship between the circle radius and the number of circles for covering the fault traces.

The results of *Matsumoto et al.* [1992] and *Hirata* [1989a] are not directly comparable, but, in general, both indicate similar fractal models of fault distribution, with a few exceptions. *Matsumoto et al.* [1992], for example, present the box plot for an area along the Median Tectonic Line that is characterized by two linear regions in the log-log plots. *Hirata* [1989a] notes that a fractal relationship was not observed in several areas and excluded those regions from his analysis. Hirata's analysis of boxcount data is restricted approximately to the 2-20 km range of scales, while the results of *Matsumoto et al.* [1992] appear to be restricted to the 1-10 km range of scales.

On the basis of outcrop scale studies of fracture patterns in the north Izu Peninsula area, *Hirata* [1989a] suggested that the fractal characteristics of fractures on the 10^{-1} to 10^{-2} m scale are similar to the larger-scale active fault patterns. Hirata's results also indicate that the fractal dimensions of active fault systems are highest in central Japan and decrease toward southwest and northeast Japan.

The general form and physical significance of spatial and temporal fluctuations of the seismic *b* value have been discussed by many authors [e.g., *Gibovicz*, 1973; *Smith*, 1986; *Main et al.*, 1990; *Öncel et al.*, 1995, 1996a, 1996b]. *Hirata* [1989b] evaluated the relationship between Gutenberg-Richter *b* value and the fractal dimension of focal point distribution. *Hirata* [1989b] found a negative correlation between the fractal dimension of focal point distributions and *b* value for the temporal variation of seismicity in the Tohoku region of Japan. A similar relationship between seismic *b* value and fractal dimension of the hypocenter distribution was obtained for the Parkfield area of California and northeastern Brazil [*Henderson et al.*, 1992, 1994]. *Öncel et al.* [1996a, 1996b] observed a strong negative correlation between the seismic *b* value and fractal dimensions of the temporal and spatial variations of seismicity in the North Anatolian Fault Zones (NAFZ). They pointed out that spatial variations of those parameters coincide with variation of geological structure or mechanical properties along the fault strike, while their temporal variations are consistent with stress intensity and greater clustering of seismicity, respectively [*Main et al.*, 1990]. On the contrary, *Öncel et al.* [1995] concluded that systematic temporal changes of the latter parameters in the western part of NAFZ can be assigned to an artificial effect rather than to underlying tectonic mechanisms because upgrades in the seismic observation network led to temporal changes of the parameters. In the discussion about the relationship between seismic *b* value and fractal dimension of focal point distributions, *Xu and Burton* [1999] pointed out the possibility that the result may depend on the earthquake magnitude range for which the analysis is undertaken. Their observations suggest that seismic *b* value varies from the macroscale (large *m*) and microscale (small *m*) regions. The macroscopic characteristics of seismicity observed in both Japan and along the NAFZ yield negative correlation between the fractal dimension of focal points and *b* value, while the microscopic characteristics of seismicity for low-magnitude events such as the cluster patterns of Brazil yield positive correlation. The observations of *Xu and Burton* [1999] suggest a scale-dependent relationship, which is based on the occurrence of changes in "fractal" properties with scale range of seismicity, in contrast to the suggestions of *Chen et al.* [1998] and *Kagan and Knopoff* [1980] where the fractal characteristics of seismicity are magnitude independent.

3. Active Fault Analysis

3.1. Active Fault Data and Region of Analysis

Active faults analyzed in this study were digitized from revised editions of active fault maps [*Research Group for Active Faults of Japan*, 1991] updated by the Geological Survey of Japan. Individual sheet maps cover 1° longitude by 40° arc min latitude areas roughly 90 by 74 km at 1:200,000 scale. The active faults represented on these sheet maps portray all faults believed to have been active during the Quaternary (last 2 Myr). Active faults are grouped into three categories depending on the certainty that movement actually occurred along any given fault during the Quaternary. In this study, we include all faults in our analysis so that our results can be compared directly to those of *Hirata* [1989a, 1989b] who undertook the first comprehensive analysis of the fractal characteristics of faulting in Japan.

In order to portray variations in the fractal properties of the active fault network of Japan and relate them to seismicity via seismic *b* value, the analysis was conducted along three lines (Figure 2) that extend along the length of Honshu. The analysis lines cross major tectonic subdivisions of Japan, and the presentation of data along these lines yields continuous profiles of variation in fractal dimension and seismicity that cross major tectonic boundaries. The western end of each line is shared by lines 1 through 3 and extends ~ 440 km from the westernmost end of Honshu east to Kyoto and then continues along three separate branches. Line 1 continues eastward to Lake Kasumi (Kasumigaura), passing through the southern part of central Honshu. Lines 2 and 3 are almost parallel, cutting through central Japan and then continuing through northeast Honshu (Tohoku region). Line 2 covers the middle part of central Honshu and the eastern part of Tohoku (Outer side of Japan), whereas line 3 covers the northern part of central Honshu and the western part of Tohoku (inner side of Japan). In northeast Honshu (Figure 2), line 2 lies to the east and line 3 to the west.

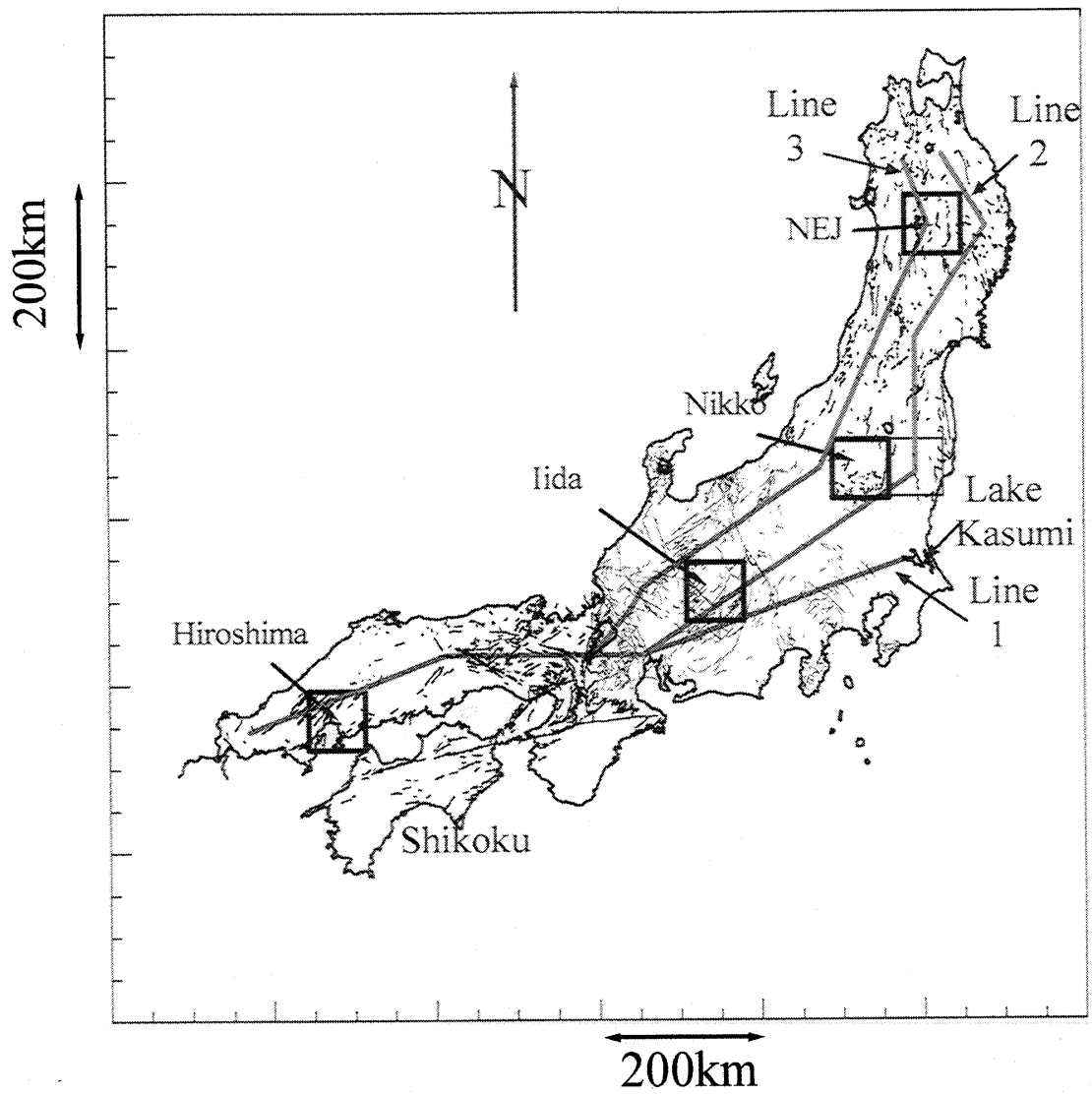

Figure 2. Active fault map of Honshu and Shikoku. The 70km x70 km Hiroshima and Iida analysis areas are located along with analysis lines 1 through 3. Reference distances are marked on the analysis lines.

Active fault analysis was conducted every 20 km along each line of 70 km x 70 km square regions centered at each analysis point. The sides of these square regions are oriented east-west and north-south. The lines were located so that the 70 km x 70 km analysis regions, in general, did not extend beyond the coastline. Thus the effects of missing data and irregular geometry are minimized. With the exception of the first 70 km of each line the covering boxes rarely extend beyond the coastline, and in those few exceptions, the initial covering box extends only a few kilometers beyond the coastline. Overlap in the area of analysis between successive analysis points also yields relatively smooth variation in calculated fractal dimension along each line.

3.2. Computation of Fractal Dimension for the Active Fault Pattern

In this study, the box counting method [e.g., *Hirata*, 1989a; *Turcotte*, 1989] is used to evaluate the detailed size scaling characteristics of active fault networks in Japan. The fault pattern is covered by square boxes with sides of length r and the number of boxes (N) containing part of the fault pattern is counted. If the pattern is fractal then the number of occupied boxes (N) varies as the length of the box side (r) raised to some power ($-D$) as shown in equation (2);

$$N = Cr^{-D}, \tag{3}$$

D is referred to as the fractal dimension and C is a constant. As defined by equation (3), D is a scale invariant parameter.

Box counting analysis is illustrated using the active fault data of Iida (location shown in Figure 2). A close-up view of the fault pattern in the Iida area is shown in Figure 3a. Log transformation of equation (2) yields a linear relationship between log N and log r with slope of $-D$. Number of occupied boxes (N) versus the box size (r) is plotted in a log-log scale (Figure 3b). Box counting of the Iida area was discussed and illustrated by *Hirata* [1989a] (see Hirata's Figure 2 for comparison). Hirata's estimate of D for the Iida area is 1.6, which was obtained from the 18.4-2.34 km range. Our estimate was made over a similar range, 17.5-2 km

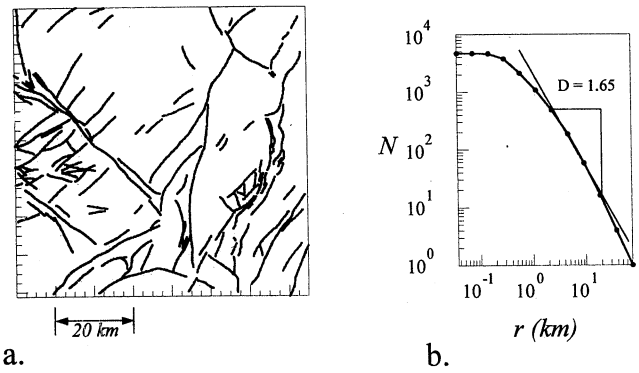

Figure 3. (a) Active faults of the Iida area located in Japan (Figure 1). (b) log *N*/log *r* plot of the active fault network in Iida.

(Figure 3b), and yielded $D = 1.65$. Hirata's analysis and that presented in Figure 3b are undertaken using a base 2 reduction in box size over the 18.4 to 2.34 km range. Thus the fractal dimension is computed from only four data points. In the current study we use a fractional box counting algorithm [see *Wilson*, 2000] that allows the size of the covering boxes to be adjusted using a noninteger base. Box size was decreased in equal logarithmic steps using a base approximately equal to 1.13. Base 1.13 decreases in box size yield 25 data points over the 17.5 to 2 km range. Recomputation of N and r from the Iida area using smaller logarithmic decreases in box size reveals significant non-linearity in the log *N*/log *r* plot of the Iida region (see Figure 4b). Two linear regions are observed (Figure 4b) with statistically different slopes of -1.88 ± 0.036 and -1.45± 0.023. Similar analysis is shown for the active faults mapped in the Hiroshima area (Figures 4c and 4d). Again, two nearly linear regions with statistically different slopes can be identified in the log *N*/log *r* plots.

3.3. Sources of Error in Box Counting Analysis

In our analysis we have been careful to avoid features of the log *N*/log *r* plots that are unrelated to the fundamental scaling properties of the pattern. For example, the initial (70 km x 70 km) box will always be occupied since it covers the entire area. In the second covering, which consists in this example of four 35 km x 35 km boxes, all boxes continue to be filled. When boxes at successively smaller scales are all occupied, the number of occupied boxes (N) increases as the square of the number of boxes along the map edge, and the number of boxes covering the map edge increases as $(1/r)^2$ yielding a log-log slope of –2 and fractal dimension of 2. The first two to three coverings of an area are commonly saturated with parts of the pattern. The steep slope (-2) observed (for example, in Figure 3b) for the larger size boxes does not accurately characterize size scaling attributes of the fault network at those scales. The first box covering counted in this analysis consists of boxes 17.5 km on a side and a total of 16 boxes. Some of the boxes usually become unoccupied at this scale.

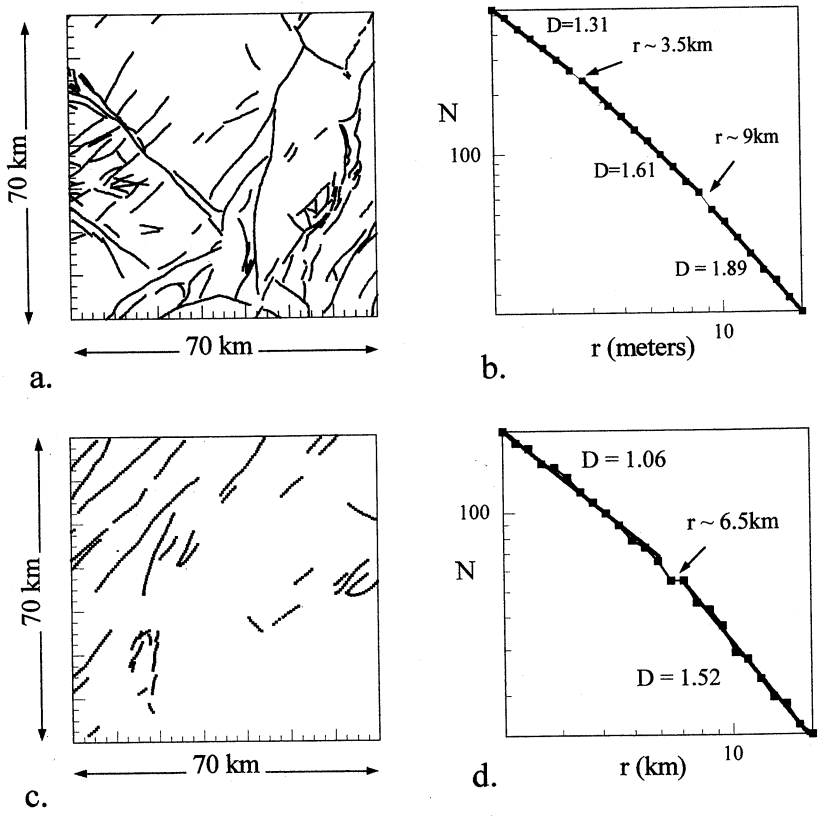

Figure 4. (a) Active faults of the Iida area located in central Japan (Figure 2). (b) log *N*/log *r* plot of the active fault network in Iida. (c) Active faults of the Hiroshima area located in southwestern Japan (Figure 2). (d) Box curve for the active faults mapped in the Hiroshima area [after *Wilson et al.*,2001a].

Regions where D approaches 0 (e.g., Figure 3b) were also avoided in this analysis. The slope of the box curve decreases rapidly when the size f the box becomes less than the sampling interval used to digitize the fault traces. In this study, fault traces were digitized at ~ 200 m intervals. For box sizes less than the sampling interval the number of occupied boxes will equal the total number of samples in the data set. Further decreases of box size yield no further increase in the number of occupied boxes and the slope of the curve in this region flattens out to 0 (Figure 3b). If the data were composed of continuous line segments, a reduction in box size by 1/2 would double the number of occupied boxes, and we would eventually end up in a nonfractal region with D approaching 1 rather than 0. The scale at which this transition occurs may represent a resolution limit below which finer details are not represented, or are, in fact, not present. Fault patterns with $D \leq 1$ [e.g., *Hirata*, 1989a] are also expected when the fault patterns appear as sets of disconnected segments which behave somewhat like the Cantor set. *Walsh and Watterson* [1993] note these issues in their reevaluation of Pavement 1000 from *Barton and Hseih* [1989] in the Yucca Mountain area. *Walsh and Watterson* [1993] note that meaningful evaluations of a pattern's size-scaling attributes must be conducted in the zone between the transitional regions noted above to avoid sources of error associated with fracture trace digitization (or bitmap representations) and box saturation in the larger box coverings. *Walsh and Watterson* [1993] suggest that fractal analysis should be confined to the range of scales between the largest and smallest fracture spacing in the data set. A spacing of a kilometer or so represents an approximate minimum spacing for the active faults in the Iida area (Figures 3a and 4a). Maximum fault spacing reaches nearly 40 km or so between some of the smaller faults in the northwest quadrant of the area (Figures 3a and 4a). However, in this case, covering boxes greater in size than 17.5 km tend to be all occupied and thus yield a fractal dimension of 2 in the large r region of the log N/log r plot. The range of box sizes (17.5 to 2 km) used in this study falls well within the range of scales accurately portrayed in the active fault maps.

3.4. Nonfractal Behavior and Scale Transitions

Prior evaluation of nonlinearity in the log N/log r plots of the active faults in Japan [*Wilson*, 1999, 2000] generally found transitions between approximately linear regions at values of r between 6 and 9 km. These transitions are reminiscent of those found by *Scholz* [1995] using a power spectral analysis of surface roughness. Scholz noted the occurrence of both gradual and abrupt transitions in the fractal dimension with spectral wavelength. In his analysis of the surface rupture produced by the Dasht-e-Bayez earthquake of 1968 in Iran, *Scholz* [1995] found an abrupt transition in fractal dimension at 10 km scales. Scholz suggests that this transition is associated with the seismogenic thickness of the crust. *Odling* [1992] also notes the presence of slope breaks in his analysis of a single fracture pattern. The break that he observed is associated with the break from a slope of 2 observed with the larger box coverings. *Odling* [1993] notes that this break occurred approximately at the average spacing in the fracture pattern that he analyzed. Recall from the discussion of error sources above that the break from a slope of 2 occurs when box sizes become small enough that they fall into the spaces between fractures or clusters in the pattern and are unoccupied. *Wilson* [1999, 2000] evaluated the fractal characteristics of numerous fracture patterns in addition to the active fault patterns of Japan and found that slope transitions are a common attribute of log N/log r plots. Model studies conducted by *Wilson* [1999, 2001a] reveal that these transitions are associated with dominant or average spacing in the pattern of fractures at different scales and that more than one transition can occur. The slopes and thus the fractal dimensions are range-limited. On the basis of the analysis of log N/log r plots from test areas, we estimate the power law coefficients or scaling parameters at two scales: one over the 17.5 to 8.5 km range and the second over the 7.75 to 2 km range. The power law coefficient over the 17.5 to 8.5 km range is referred to as D_L and that over the 7.75 to 2 km range is referred to as D_S. We follow the variations in D_L and D_S over these two scales and evaluate statistical relationships between the two along the entire length of Japan.

Analysis of the log N/log r response over the 17.5 to 2 km region in several areas throughout Japan (for example, Figure 4) on average yielded slope transitions around 8 km. The 17.5 to 8.5 km and 7.75 to 2 km ranges provide a satisfactory representation of slope differences encountered in test areas. The correlation coefficients of regression lines fit to the data in these regions are all 0.99 or higher. *Lei and Kusunose* [1999] also identify two nearly linear regions in the log N/log r plots computed in their analysis of active fault networks of Japan. In their analysis they divided Japan into three areas. The analysis regions were ~550 km on a side and include extensive blank areas beyond the coastline and region of mapped faults. Transitions found in their analysis were located at ~13 km. However, it is difficult to compare their transition to that observed in the current analysis. The larger area of analysis and presence of extensive blank areas may account for the differences in the location of transitions observed in their log N/log r plots.

3.5. Regional Variations in Power Law Coefficients of the Active Fault Network

The general patterns of variation in D_L and D_S throughout Japan are illustrated for line 2 (Figure 5a). On all three lines taken together, D_L is on average 0.33 higher than D_S. Increases and decreases of the power law coefficients along each line follow the increases and decreases in the intensity of faulting or total length of fault trace in any given analysis area. This is anticipated since the total line length (L) at a given scale (r) is just Nr. Substitution of N from equation (3) yields $L = Cr^{1-D}$. From this relation, we find that the ratio of the length of fault traces (L_2) measured at scale r_2 to L_1 measured at scale r_1, grows as $(r_1/r_2)^{D-1}$; r_1 is the initial box size so that the ratio r_1/r_2 is always greater than 1.

Southwestern Honshu is relatively narrow, and the analysis in this area was confined to one segment to prevent the 70 km x70 km analysis areas from extending beyond the coastline. In westernmost Honshu from 0 to 260 km (e.g., Figure 5)

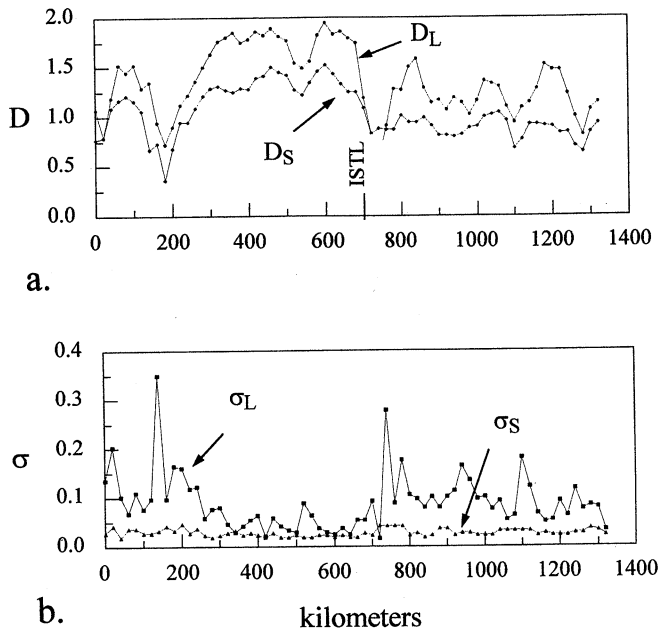

Figure 5. Figure 5: A) Range-limited fractal dimensions D_S and D_L are compared. B) Standard deviations σ_S and σ_L in the estimates of D_S and D_L, respectively, are compared.

average D_L is 1.16. Average D_S in this same area is only 0.89. From 260 to 440 km $\langle D_L \rangle$ increases to 1.71 and $\langle D_S \rangle$ increases to 1.16. At both scales, the differences between D_L and D_S in these two areas of western Honshu are statistically significant at α=0.01 level based on the non-parametric Kolmogorov-Smirnov test. The power law coefficients of active fault patterns over the 17.5 to 8.5 km scale range (D_L) remain high with an average of 1.72 in central Japan west of Itoigawa-Shizuoka Tectonic Line (ISTL) but drop to an average of 1.26 east of the ISTL. This difference is also significant at the α=0.01 level. Average D_L in northern Honshu drops further to 1.19. While $\langle D_L \rangle$ in northern Honshu is less than that east of ISTL in central Japan, the difference is generally not statistically significant. The difference approaches significance (α=0.1) only when compared to D_L east of ISTL on line 1. Here D_L rises to 1.29.

Variations in D_S continue to follow D_L. Across the ISTL, D_S drops from an average of 1.34 to 1. The decrease continues into northeast Honshu where D_S drops to 0.88. Differences in D_S across the ISTL are significant at α=0.01. Differences in D_S between northeast Honshu and the region east of the ISTL in central Honshu are also significant at α=0.01 except for the region east of ISTL on line 2. The region east of the ISTL (e.g., Figure 5) is a transitional region on all lines where D_L and D_S decrease in value. Along line 2 the decrease is more abrupt so that D_L and D_S in this area differ little from those in northeast Honshu.

3.6. Error Analysis of D_L and D_S

Standard deviations in the estimates of D_L and D_S are compared for line 2 (Figure 5b). On average, the standard deviations in the estimates of D are 0.03 for D_S and 0.09 for D_L. Standard deviations for D_S are fairly constant as shown for line 2 (Figure 5b), whereas those for D_L are quite variable. The standard deviations for estimates of D_L are much higher in the less intensely faulted areas of northeastern and southwestern Japan. Similar results are obtained along lines 1 and 3. D_S is a more stable estimate than D_L. The 95% confidence limits on the estimates of D_L and D_S are on average, 0.21 and 0.6, respectively. Given an average difference of 0.33 between D_L and D_S the confidence limits on D_L and D_S make them on average statistically different at the 95% confidence level. In the remainder of this study we compare b values only to D_S, since the precision of D_S, on average, is ~ 3 times that of D_L.

4. Earthquake Magnitude Analysis

Figure 6 shows the frequency-magnitude relation of events along lines 1-3 for magnitudes > 2.5. In Figures 1 and 6, lines 1 and 3 include a large number of great events with magnitudes 7 or greater. Along line 2, which passes through central Japan and then goes out along the outer (east) side of northern Japan, there are few events with the magnitude >7. One possible interpretation of this difference is that the recurrence time of large earthquakes with magnitude greater than 7 may be longer than 400 years in the areas traversed by line 2, since the time span of available data is only 400 years.

The analysis of earthquakes in this study was restricted to the zone of intraplate seismicity at depths ≤20 km. The thickness of the seismogenic zone in Japan is estimated to be ~15-20 km [*Shimazaki*, 1986]. Deep-seated earthquakes at depths > 20 km are most certainly linked to the interaction of the subducting plates of the northeast and southwest Japan rather than intraplate faulting. The database used in this study was extracted from three earthquake databases including historical events: (1) *Usami*'s [1996] historical catalogue from 1600 to 1884, (2) *Utsu*'s [1982] catalogue for the time period between 1885 and 1925 and (3) the instrumental catalogue compiled from the Japan Meteorological Agency (JMA) data file for the time period between 1926 and 1997. The compilation of the long-term seismic activity of Japan covering the past 400 years is considered to be complete [*Kijko and Oncel*, 2000]. Figure 1 shows the hypocenter distribution.

The magnitude scale of historical data was taken from *Utsu* [1982] and *Usami* [1996] since they converted estimates of the magnitudes of historical events to the magnitude scale of JMA catalogue (T.Kumamato, personal communication, 1998). We do not know the depths of these historical events but differentiate between intraplate and interplate events based on reports of damage associated with these events.

Only the main shocks, as selected by the *Gardner and Knopoff*'s [1974] procedure, were used in this analysis for a more reliable estimation of seismicity parameters (Oncel and Alptekin, 1999). The completeness for *Usami*'s [1996] historical earthquake catalogue contains only the largest events (with M magnitudes > 7.0) and provides information about long-term seismicity during the period from January 1, 1600 to December 31, 1884. The completeness for *Utsu*'s [1982] catalogue includes all events of the magnitude ≥ 5.7. More recent seismicity data are taken from the JMA database.

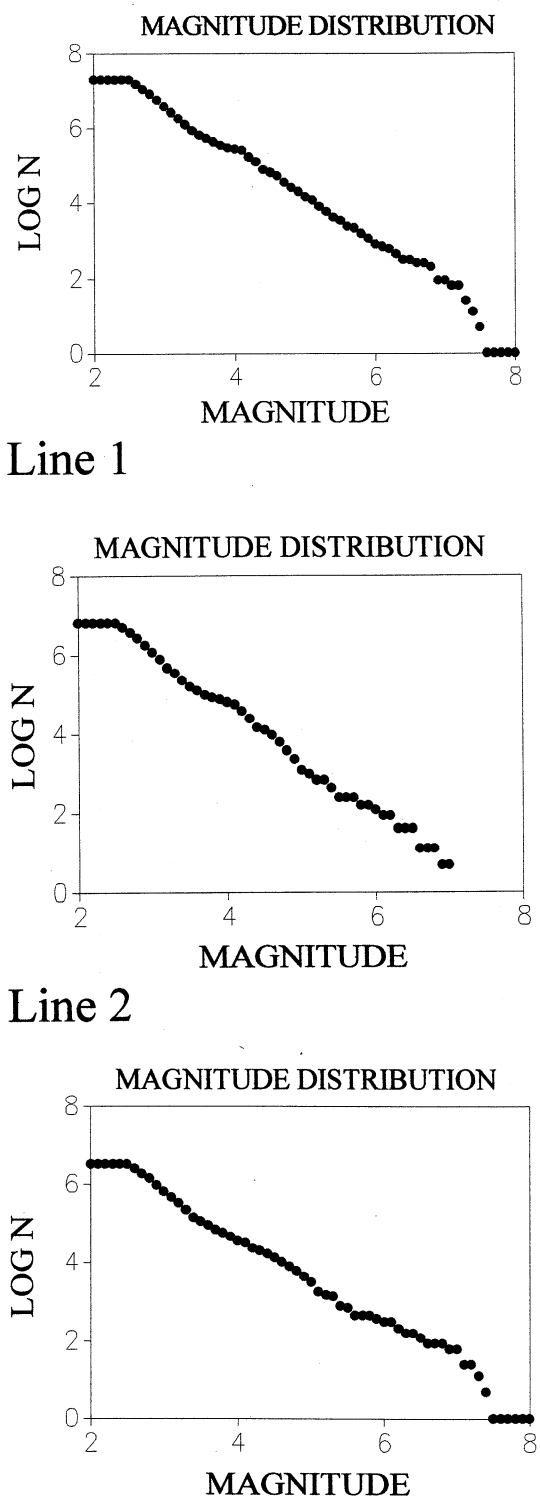

Figure 6. Frequency-magnitude distributions for 100 km-wide bands of seismicity centered on each of lines through 1 to 3.

The JMA database is divided into three subsets covering the period of time from January 1, 1926 to December 31, 1997. Data during the period extending from January 1, 1926 to December 31, 1977, includes complete coverage of earthquakes with magnitude ≥ 4.1. The second part of the JMA catalogue (from January 1, 1978, December 31, 1988) includes all earthquakes of magnitude ≥ 2.8. The third part of the JMA catalogue (from January 1, 1988, to December 31, 1997) gives complete coverage of earthquakes with magnitude ≥ 2.5.

5. Method of Analysis

5.1. Seismic *b* Value

Seismic b value is calculated using the maximum likelihood methodology by the use of unequal completeness periods for different magnitude thresholds [e.g., *Kijko and Sellevoll*, 1992, *Oncel et al.*, 1996a, 1996b]. Seismic b value may be estimated by the use of different methodologies such as maximum likelihood and least square. In this study, the maximum likelihood methodology (MLM) is preferred to compute seismic b value because it is reported to be a more appropriate way to compute a better estimation of b value since it is inversely proportional to the mean magnitude [*Utsu*, 1965; *Aki*, 1965]:

$$b = \frac{\log_{10} e}{\overline{m} - m_0}, \tag{4}$$

where $\overline{m}$ is the average magnitude of events exceeding a threshold magnitude (m_0) for complete reporting of earthquake magnitudes and $\log_{10} e = 0.4343$. A stable estimation of the b value by the MLM requires at least 50 events [*Utsu*, 1965]. The standard deviation (δb) of seismic b value in 95 % confidence limits may be determined using the equation suggested by *Aki* [1965]:

$$\delta b = 1.96 b / \sqrt{n}, \tag{5}$$

Estimates of b value were made in cylindrical volumes of radius r equal to 50 km and height h equal to 20 km. The centers of each cylindrical region were positioned at 20 km intervals along each of the three lines (Figures 1 and 2). Seismic b value was calculated for each volume along the profile.

5.2. Variations of *b* Value

The increase and decrease of b values along each line in general follow the visual density of the seismicity pattern (Figure 1). In westernmost Honshu from 0 to 260 km along line 1 (e.g., Figure 7a) the average b is 0.62±0.06. From 260 to 440 km <b> decreases to 0.51±0.04. In south central Japan from 500 to 800 km along line 1 b drops further to 0.49±0.05. The b values on line 1 from 820 to 840 km have higher standard errors (~0.4 and 0.5) since the number of events in this area is <10. Average b through central Japan on line 2, from 500 to 900 km (Figure 7b), is 0.64 ± 0.06. On line 3 (Figure 7c) <b> drops to 0.56 ± 0.05 through north central Japan.

Seismic b values computed in this study may have possible artifacts associated with systematic temporal variations in the pattern of earthquake location and station coverage that is difficult to assess. However, any such fluctuations are likely to have affected the results in a similar way for each profile, and we have attempted to minimize such artifacts by choosing largest events, which are more likely to be completely reported. In the present comparative study the effect of any

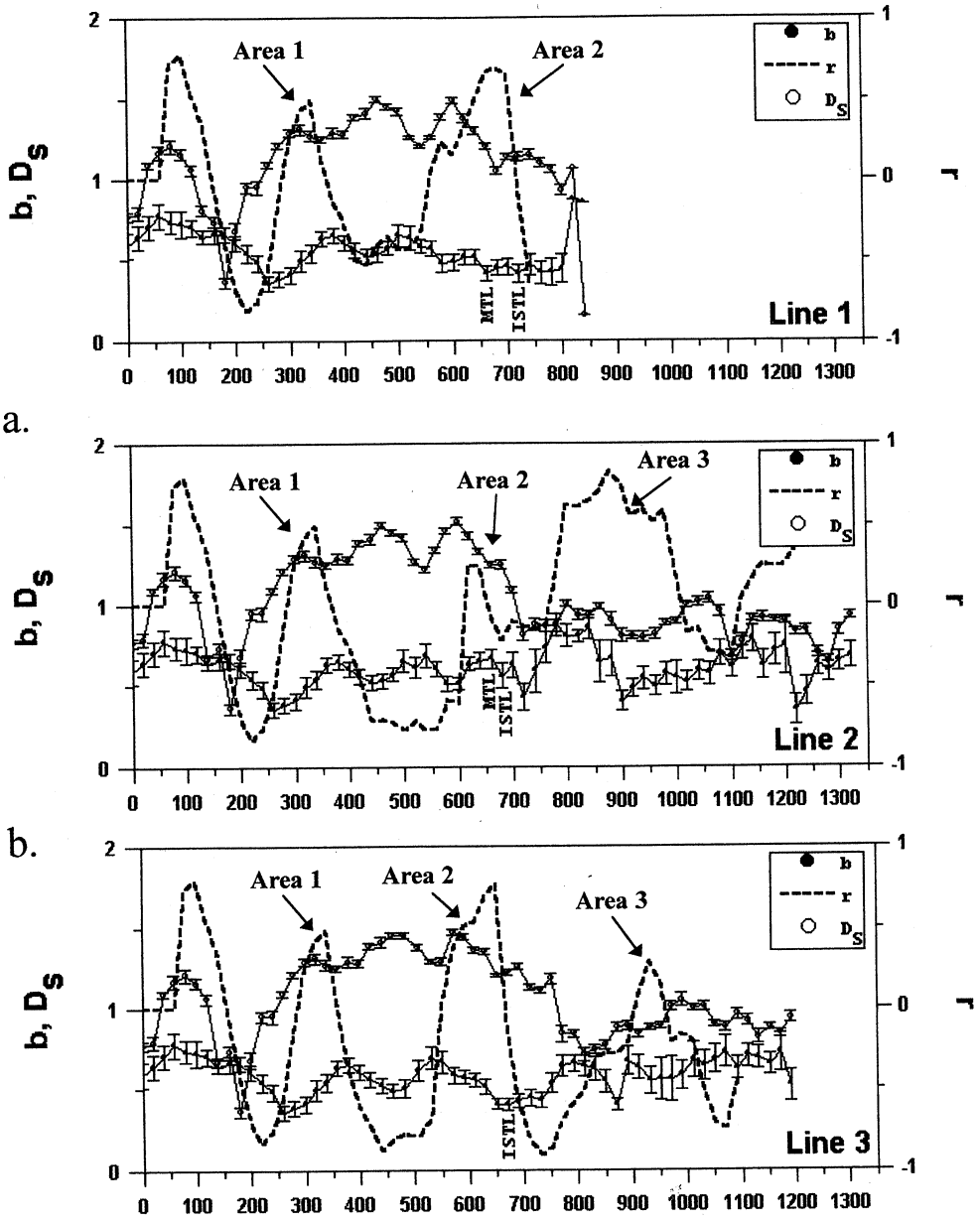

Figure 7. Variations in b and D_S along lines 1 -3. MTL, Median Tectonic Line. ISTL, Itoigawa Shizuoka Tectonic Line. The dashed line shows variations in the local correlation between b and D_S. (a) Line 1 ending in central Japan. (b) Line 2 extending along the entire length of Honshu. (c) Line 3 extending along the entire length of Honshu. Area 1 through 3 are labeled.

such artifacts is therefore more likely to affect the absolute values of the parameters rather than their relative values.

5.3. The *b* Value Error Analysis

Standard deviations in the estimates of b value are compared for each line (Figure 6b). The standard deviations in the estimates of b, are on average, 0.05 for line 1, and 0.06 for lines 2 and 3. Standard deviations for b value are fairly constant along the length of line 2. The standard deviations for estimates of b value are much higher in the less seismically active areas of northeastern and southwestern Japan, but the differences, on average (0.01), are not so significant.

5.4. Correlation Analysis Between *b* Value and Fractal Dimension

Gutenberg-Richter b value is used to define changes of seismicity observed along each analysis line. In general, regions characterized by high b value have a greater proportion of low-magnitude earthquakes, while areas of low b value represents areas where large magnitude earthquakes are more likely. Areas in the active fault network characterized by higher D are associated with greater complexity in the fault pattern and a persistence of this complexity at smaller scales. As noted earlier, increases in D are, in general, related to increases in the total length of faults over the 7.5 to 2 km scale.

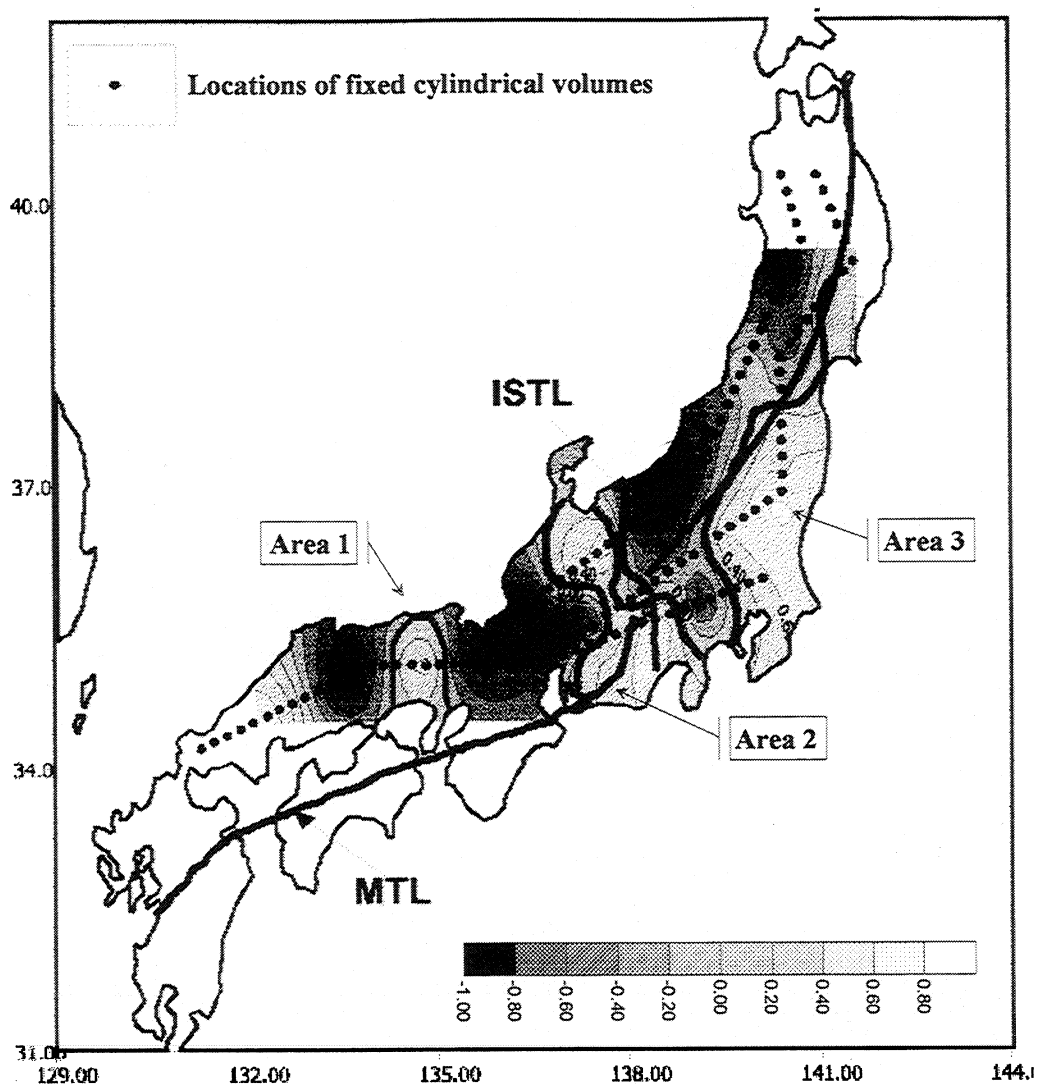

Figure 8. Correlation coefficients between b and D_S computed along lines 1-3 are contoured to illustrate the spatial distribution of positive correlation regions (areas 1-3) throughout Japan. Areas 1, 2 and 3 are identified.

Comparison of Gutenberg-Richter b values and D_S along lines 1-3 yields negative correlation. The correlation coefficient between b and D_S along line 1 is -0.35. Along lines 2 and 3, the correlations are -0.12 and -0.33, respectively. Examination of Figure 7 reveals that increases in D_S are often associated with decreases in b value. We suggest that a negative correlation is in general, to be expected for the following reasons. A decrease in b is associated with increased probability of larger magnitude earthquakes, while increases of D indicate increased fault length. The general tendency for b to decrease when D_S increases suggests that there is increased probability that stress release will occur with through rupture along faults of greater length and therefore greater surface area. Figure 7 reveals that there is considerable spatial variability in the relative changes of b and D_S. We wished to evaluate this relationship at a more local level throughout Japan to determine if variations in the correlation might be related to the major tectonic subdivisions in Japan. To do this, we compared D_S and b along lines 1-3. Correlation coefficients between D_S and b were computed at 20 km intervals along each line. As noted, b was computed from seismic events located in cylindrical regions with radius of 50 km and depth of 20 km. D_S was computed at the same points from active faults in 70 km x 70 km size square regions. Although the analysis is presented along lines, the data are representative of large areas and volumes centered on each line.

A local measure of the correlation between b and D_S was computed using a 160 km-long sliding window. The local correlation is plotted along each line in Figure 7 and is contoured in Figure 8. The local correlation (Figures 7 and 8) reveals large regions of negative and positive correlation throughout Japan (Figure 8). One zone of positive correlation (area 2) extends north-south through central Japan (Figure 8). Just to the east, across the ISTL, this zone of positive correlation changes abruptly to a zone of low correlation. The ISTL marks the location of an incipient subduction zone between the Eurasian plate (to the west) and the North

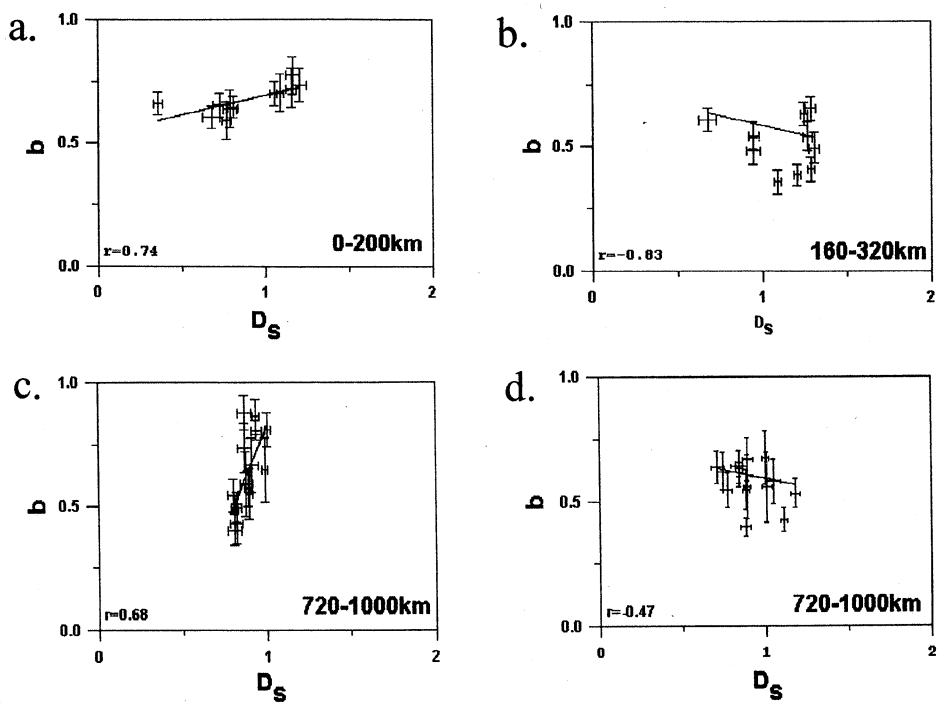

Figure 9. Areas of positive correlation between D_S and seismic b value on a more local scale. Cross plots are shown for intervals along line 1 that extend from (a) 0 to 200 km, (b) 160 to 320 km and intervals along (c) line 2 and (d) line 3 that extend from 720 to 1000 km.

American plate (to the north). The area west of the ISTL in central Japan coincides with the most intense concentration of Quaternary faults [*Wesnousky et al.*, 1984] (also see Figure 2).

These 160 km windows of data included nine data points. Examples of the relationship between D_S and b are illustrated in Figure 9. The examples are taken form positive correlation areas 1, 2 and 3. In section 6 we examine the different areas of positive and negative correlation and consider their statistical as well as seismotectonic significance.

6. Discussion

The comparison of b value to D_S reveals regions of both positive and negative correlation (Figure 8). These regions are extensive and in central Japan reveal consistency from line to line. In the following discussion we consider the possible significance of the correlations beginning first in southwestern Japan and proceeding through central Japan into northeastern Japan.

A small region of positive correlation appears on the southwestern end of line 1. The correlation occurs in response to a parallel rise and fall in the value of D_S and b along the first 100 km of the line (Figure 7). D_S varies from ~ 0.8 to 1.2. Standard deviations of the estimates of D_S are 0.03. The variation in D_S exceeds the standard deviation in the estimate over 13 times and is considered significantly different. The variation of b through this region is at most 0.2. Standard deviation in the estimate of b in this area is ~ 0.1. The 0.2 variation in b differs by at most two standard deviations. The fluctuations in b are however, quite variable, and the resulting correlation between D_S and b cannot be considered significant.

To the east at ~200 km along line 1 the correlation coefficient drops to approximately -0.8. This zone of negative correlation develops in response to an increase in D_S and a parallel decrease in b value. In this case the drop in b is ~0.45. The standard deviations of the estimates of b in this area are approximately 0.05, so that the drop in b value is considered significant. The variations in D_S also form a statistically significant positive trend. Excluding the extremely low value of D_S (0.3) at ~ 160 km out along the line, D_S increases ~ from 0.7 to 1.1 (13 standard deviations). Since the rise and fall of D_S and b (respectively) are statistically significant, the negative correlation that arises around 200 km is also considered statistically significant.

The drop in b implies a relative increase in the probability of larger-magnitude earthquakes [Oncel and Wyss, 2000). The decrease in b with increase in D_S suggests that in this increasingly deformed area, fault planes may have greater surface area and give rise to earthquakes of greater magnitude. However, maximum earthquake magnitudes in this area (see Figure 10) tend to be on average about 6. The coincidence of increased fault complexity with lower b value and relatively low historic earthquake magnitudes suggests that there may be increased probability of larger-magnitude earthquakes occurring in this area.

Continuing farther to the east, we examine the west-to-east rise in the local correlation observed through area 1 (see individual line plots, Figure 7). On line 2, for example, D_S increases from ~ 0.7 to 1.25 through the region of positive correlation. Given the relatively low standard deviation in the estimates of D_S and b, this region of positive correlation is considered significant. The rise in D_S indicates increased

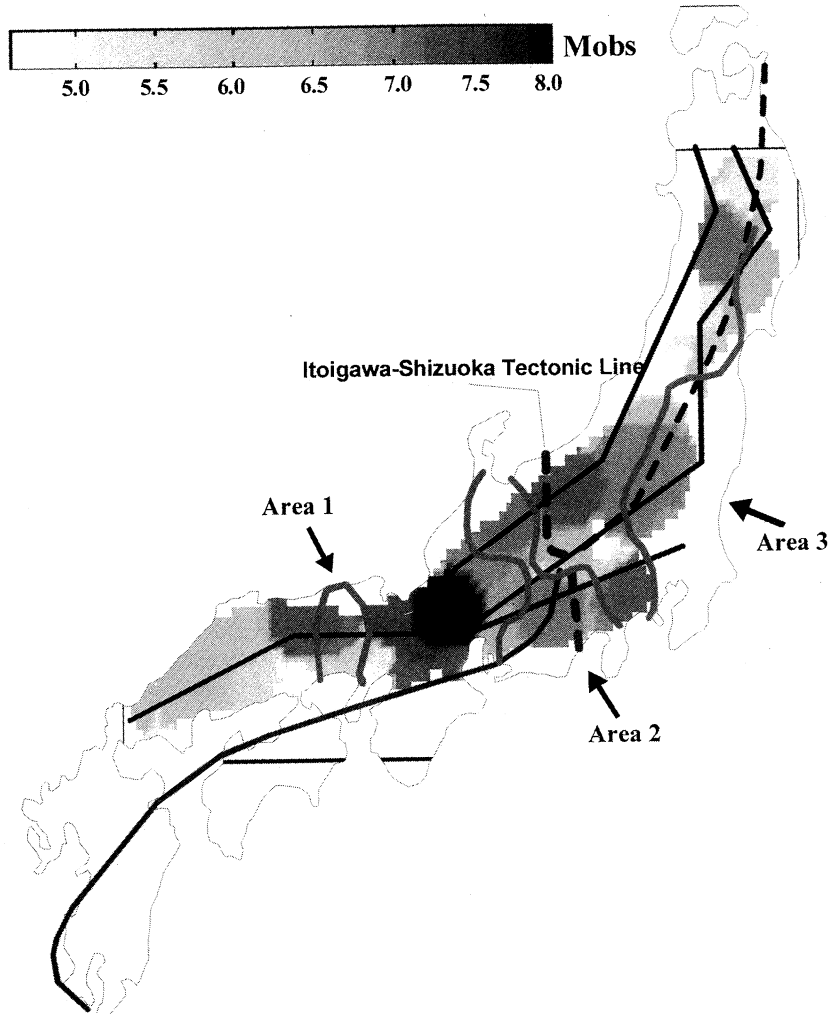

Figure 10. Map shows the distribution of maximum observed earthquake magnitude throughout Japan and locations of positive correlation areas 1 through 3.

complexity in the active fault complex. The concomitant rise in b suggests decreased probability of higher-magnitude earthquakes. Earthquake magnitudes in the area are again ~ 6 on average. In this case, an increasingly complex active fault network may accommodate stress release on faults of smaller surface area.

Positive correlation in area 2 (Figure 8) develops from an east-to-west rise in both b and D_S. The east-to-west rise in D_S is significant on all three lines (see Figure 7). The significance of the rise in b is questionable on lines 1 and 2, but the 0.4 to 0.7 rise in b value along line 3 from 650 to 500 km is significant. The significance of the positive correlations in the southern part of area 2 may be questionable, but the correlation in the northern part of area 2 is not. In general, these positive correlations appear to be associated with transitions from sparse to dense areas in the active fault network accompanied by decreased probability of larger magnitude earthquakes. Area 2 coincides with areas where the maximum earthquake magnitude is generally lower than in surrounding areas (Figure 10) and provides support for the lowered probability of larger earthquakes. The coincidence between increased complexity in the active fault network and lowered probability of larger earthquakes suggests that as in area 1, stress release is accommodated on faults of smaller surface area.

Between areas 1 and 2 we find an area of negative correlation extending from about 350-600 km on all three lines (Figures 7 and 8). The west-to-east decrease in b between 375 and 475 km on line 3, for example, is from ~ 0.7 to 0.45. D_S increases from ~ 1.25 to 1.45. In both cases, the change is significant over this region of negative correlation. The differences in b observed to the south on lines 1 and 2 are smaller and of questionable significance. We consider the northern extent of the negative correlation area along line 3 to be significant. The decrease of b into the center of the area suggests an increased probability of higher magnitude earthquakes. Examination of the active fault complex in Figure 2 indicates that the region of negative correlation is associated with an intensely faulted area between the 400 and 500 km markers (Figures 2 and 7). Note that the areas west and east of this 400-500 km area are less intensely faulted and associated with a reduction in D_S to either side of the point located at 450 km in lines 1 through 3 (see individual line plots in Figure 7). Stress may be concentrated in this more intensely faulted area, giving rise on average to higher-magnitude earthquake activity. An increased probability of

large earthquakes in this area is confirmed in Figure 10 where larger-magnitude earthquake activity forms a distinct trend that coincides with this area of negative correlation (Figure 8).

The area of negative correlation lying just east of the ISTL arises from significant differences in b and D_S along lines 2 and 3. D_S increases from the east toward the ISTL as b decreases. The decrease in b suggests that there should be increased probability of larger magnitude earthquakes. Examination of Figure 10 confirms that the maximum magnitude of earthquakes in this region is slightly greater than area 2 just to the west.

A third zone of positive correlation (area 3) is observed along line 2 in northeastern Japan. The positive correlation between 775 km and 975 km is loosely associated with a parallel rise and fall of D_S and b centered at about 800 km along the line (just west of 900 km mark on Figure 2). The rise and fall of b in this area (see Figure 7) is significant, but the variations of D_S (0.1 at most) are quite small and of questionable significance. In general, throughout this region of positive correlation, the variations of D_S are small and erratic and we do not consider it further. Other regions of positive and negative correlation appearing farther to the north along lines 2 and 3 (Figure 7 and 8) lack statistical significance and are not discussed.

7. Summary and Conclusion

We have analyzed seismicity data covering a period between 1600 and 1997 to examine the spatial variations of the Gutenberg-Richter b value and the size scaling attributes of the active fault networks observed along three lines (Figure 2) that extend along the length of Honshu, Japan. We used the methods of box counting and maximum likelihood for analyzing the complexity of the fault network and the rate changes of seismicity, respectively.

Detailed box counting of the active fault patterns in Japan over the 17.5 km to 2 km range yields two linear regions in the log N and log r box curve. These linear regions are separated by an abrupt transition located at ~ 8 km scales. The nonlinear behavior over the 17.5 to 2 km scale range indicates that the fault network is not truly fractal or possesses only range-limited fractal properties. We were careful to avoid possible sources of error associated with data sampling and box saturation in the larger box coverings. The range-limited fractal dimension or power law coefficient over 17.5-7.5 km scale (D_L) is almost always statistically greater than the range-limited fractal dimension computed over the 7.5-2 km scale (D_S). The standard deviations in the estimates of D_S (0.03) are considerably less than those for D_L (0.09) so that D_S was used to represent the variations in complexity of the active fault network.

Overall there is a negative correlation between the Gutenberg-Richter b value and the active fault size scaling parameter (D_S) along each of the three profiles. The correlations between D_S and b on lines 1 ~ 3 are -0.35, -0.12, and -0.33, respectively. Negative correlation between b and D_S suggests that increases in the complexity of the active fault network (higher D) are, on average, associated with increased probability of occurrence of larger-magnitude earthquakes (lower b) and vice versa. This relationship suggests that increased fault complexity (increased D_S) increases the interconnections between faults and thus increases the total fault surface area along which fault rupture can occur. In general, the larger the fault rupture area, the larger the magnitude of the earthquake [e.g., *Turcotte*, 1997].

Computation of local correlation between b and D_S using a sliding 160 km long window reveals that negative correlation does not persist at more local scales (Figures 7 and 8). Regions of local positive and negative correlation are observed. We suggest that positive correlation areas 1 and 2 (see Figure 8) occur when fault complexity (larger D_S) becomes so great that it is possible to accommodate stress release on smaller faults. It becomes increasingly unlikely in these areas that fault rupture will occur along one, through-going fault surface. The fault network is too fragmented.

The net result is that these areas, which are exceptions, are characterized by relatively lower magnitude seismicity. One additional area of positive correlation (area 3) was also observed in the data. Although significant variations of b occur through this area, in general, we discount the significance of this positive correlation area because the variations of D_S are relatively small and erratic.

The negative correlations occurring in southwest and across the ISTL in central Japan result where b decreases along with an increase in D_S. These relative changes would appear reasonable on a tectonic basis. It seems likely that as the fault system varies spatially from a relatively sparse and fragmented network ($D_S < 1$) to one in which the faults become more continuous and numerous ($D_S > 1$), that the probability of larger earthquakes will increase (smaller b value). The possibility of rupture occurring on fault planes of larger surface area will increase with D_S but only to a certain point. Further increases in D_S, as occur in areas 1 and 2, are associated with increases in b. In these cases, the fault network may be so interconnected that the likelihood of failure along large surface area is diminished. More intensely deformed areas provide an abundance of smaller faults along which strain can be dissipated so that the probability of larger-magnitude earthquakes decreases.

The foregoing comparisons yield a measure of the correlation of short-term seismicity, represented by b value with long term deformation, represented by D_S. The possible tectonic meaning of these areas of positive and negative correlation is speculative. However, we have been able to show that present-day seismicity as measured through b value changes significantly over distances of 100-200 km and that these changes correlate negatively or positively with the changes in the distribution of active faults. Our observations suggest that examination of detailed variations in the correlation between b and D may provide insights into seismic hazard assessment of active tectonic areas. The negative correlation occurring just west of area 1 is associated with relatively low maximum magnitude earthquake activity. Yet this area has lower b values than elsewhere in Japan and coincides with an area of increased active fault complexity. The lower maximum magnitudes of earthquakes in this area may represent anomalous conditions. The coincidence of low maximum magnitude

and low *b* value may in itself suggest that historical earthquake activity in this area may not be representative of the potential for greater earthquakes. However, an active fault network of increasing complexity is present through the area along which larger-magnitude earthquakes could occur.

Acknowledgements. We are grateful to K. Kano, A.Tanaka, H.Kato and A.Kijko for their review of the paper and constructive comments. The comments of Didier Sornette and anonymous reviewers are also greatly appreciated. We would also like to thank S. Wiemer for providing us the software of ZMAP that was effectively used for the computation of seismic b value. This study was supported in part through AIST (Öncel) and STA (Wilson) fellowships. The size scaling analysis of active fault networks presented in this paper was supported in part through U.S. Department of Energy grants DE-FG21-95MC32158 and DE-FG26-98FT40385. Discussions with Tom Mroz, Royal Watts, and Bill Gwilliams of the Morgantown Federal Energy Technology Center were also much appreciated.

References

Aki, K., Maximum likelihood estimate of b in the formula log $N = a - M$ and its confidence limits, *Bull. Earthquake. Res. Inst. Univ. Tokyo, 43*, 237-239, 1965.

Aki, K., A probabilistic synthesis of precursory phenomena, in *Earthquake Prediction: An International Review, Maurice Ewing Ser.*, vol. 4, edited by D. W. Simpson and P. G. Richards, pp. 566-574, AGU, Washington, D.C., 1981.

Barton, C. C., Fractal analysis of scaling and spatial clustering of fractures, in *Fractals in the Earth Science*, edited by C.C. Barton and P. LaPointe, pp. 141-178, Plenum, NewYork, 1995.

Barton, C. C., and P.A. Hseih, Physical and hydrologic flow properties of fractures; *Field Trip Guidebk.*, vol. T385, AGU, Washington, D. C., 1989.

Chen, Y., L. Chen., and R. Wu, A new fractal apporoach to the clustering of earthquakes: physical fractal, *Bull. Seismol. Soc. Am., 88*, 89-94,1998.

Gardner, J.K., and L. Knopoff, Is the sequence of earthquakes in southern California, with aftershocks removed, poissonian?, *Bull. Seismol. Soc. Am., 64*, 1363-1367, 1974.

Hirata, T., Fractal dimension of fault systems in Japan: Fractal Structure in rock fracture geometry at various scales, *Pure Appl.Geophys, 131*, 157-170, 1989a.

Hirata, T., Fractal dimension of fault systems in Japan: Fractal Structure in rock fracture geometry at various scales, *J. Geophys. Res, 94*,7507-7514,1989b.

Henderson, J.R., I.G. Main, P.G. Meredith, and P.R. Sammonds, The evolution of seismicity at Parkfield, California: Observation, experiment, and a fracture mechanical interpretation, *J. Struct. Geol., 14*, 905- 914, 1992.

Henderson, J.R., I.G. Main.,M. Takaya, and P.R. Pearce, Seismicity in north-eastern Brazil - Fractal clustering and the evolution of the *b* value., *J. Geophys. Int, 116*, 217-226, 1994.

Kagan, Y. Y., and L. Knopoff, Spatial distribution of Earthquakes: The two point correlation function, *J. Geophys. R. Astron. Soc., 62*, 303-320, 1980.

Kato, H., Fossa Magna - A masked border region separating southwest and northeast Japan: *Bull. Geol. Surv., 43*, 1-30, 1992.

Kijko, A. and A.O. Oncel, Probabilistic seismic hazard maps for the Japanese islands, *Soil. Dyn. Earth. Eng.*, 20,485-491, 2000.

Kijko, A. and M.A. Sellevoll, Estimation of earthquake hazard parameters from incomplete data files, Part II, Incorporation of magnitude heterogeneity, *Bull. Seismol. Soc. Am., 82*, 120-134, 1992.

Kobayashi, Y., On the initiation of the subduction of plates, *Earth Mon., 5*, 510-514, 1982.

Lei, X., and K, Kusunose, The fractal structures and characteristic scale of earthquakes, active faults, rivers and topographic relief of Japan, *Geophy. J.Int., 139*, 754-762, 1999.

Main, I.G., Damage mechanics with long – range interactions: Correlation between the seismic *b*-value and the two point correlation dimension. *J. Geophys. Int., 111*, 531-541,1992.

Main, I. G., P.G. Meredith., P.R. Sammonds, and C. Jones, Influence of fractal flaw distributions of rock deformation in the brittle field, in *Deformation Mechanisims, Rheology and Tectonics*,edited by R.J. Knipe., and E.H. Rutter, *Geol. Soc.* Spec. *Publ., 54*, 81-96, 1990.

Main, I.G., P. G. Meredith., and P. R. Sammonds, Temporal variations in seismic event rate and *b*-values from stress corrosion constitutive laws, *Tectonophysics, 211*, 233-246, 1992.

Matsumoto, N., K. Yomogoda., and S. Honda, Fractal analysis of fault systems in Japan and the Philippines, *Geophys Res. Lett., 19*, 357-360, 1992.

Mogi, K., Magnitude - frequency relation for elastic shocks Accompanying fractures of various materials and some related Problems in earthquakes, *Bull. Earthquake. Res. Inst., Univ. Tokyo, 40*, 831-853, 1962.

Nakamura, K., Possible nascent trench along the Japan Sea as the convergent boundary between the Eurasian and North American plates, *Bull. Earthquake. Res. Inst., Univ. Tokyo*, 58, 711-722, 1983.

Odling, N.E, Network properties of a two dimensional fracture pattern, *Pure Appl. Geophys.,138*, 95-114, 1992.

Okubo, P., and K. Aki, Fractal geometry in the San Andreas fault System, *J. Geophys Res., 92*, 345-355, 1987.

Oncel, A.O., and O. Alptekin, Effect of aftershocks on earthquake hazard estimation: An example from the north Anatolian fault zone, *Natural Hazards., 19*, 1-11, 1999.

Oncel, A.O., and M. Wyss, Major asperities of the 1999 M7.4 Izmit Earthquake by the microseismicity of the two decades before it, *J. Geophys. Int., 143*, 501-506, 2000.

Oncel, A.O., O. Alptekin, and I. Main,Temporal variations of the fractal properties of seismicity in the western part of the north Anatolian fault zone: Possible artifacts due to improvements in station coverage, *Nonlinear Processes Geophys., 2*, 147-157, 1995.

Oncel, A.O., I. Main., O. Alptekin, and P. Cowie, Spatial variations of the fractal properties of seismicity in the Anatolian fault zones, *Tectonophysics, 257*, 189-202, 1996a.

Oncel,A.O., I. Main, O. Alptekin, and P. Cowie, Temporal variations of the fractal properties of seismicity in the north Anatolian fault zone between 31°E and 41°E, *Pure Appl. Geophys., 146*, 147-159, 1996b.

Oncel, A.O., O. Alptekin, and H. Koral, The Dinar earthquake of October 1, 1996 (M_w=6.2) in southwestern Turkey and earthquake hazard of the Dinar-Çivril fault, *Pure. Appl. Geophys, 152*, 91-105, 1998.

Otsuki, K., Oblique subduction, collision of microcontinents and subduction of oceanic ridge: Their implications on Cretaceous tectonics of Japan, *Island Arc, 1*, 51-63, 1992.

Research Group for Active Faults of Japan., Active faults in Japan: Sheet Maps and inventories, (in Japanese) rev. ed., 363 pp., Univ. of Tokyo Press, Tokyo, 1980.

Research Group for Active Faults of Japan., Active faults in Japan: Sheet maps and inventories: (in Japanese), rev. ed., 437 pp., Univ. of Tokyo Press, Tokyo, 1991.

Research Group for Active Faults of Japan., Maps of active faults in Japan and explanatory text, Univ. of Tokyo Press, Tokyo, 1995.

Research Group f or Active Tectonic Structures in Kyushu, Active Tectonic structures in Kyushu, Japan (in Japanese), 553pp, Univ. of Tokyo Press, Tokyo,1989.

Research Group for Quaternary Tectonic Map, Quaternary tectonic map of Japan., map and explanatory text, 167 pp., Natl. Res. Cent. for Disaster Prevent., Tokyo, 1973.

Scholz, C.H.,The frequency-magnitude relation of microfracturing in rock and its relation to earthquakes, *Bull. Seismol. Soc. Am., 58*, 399-415, 1968.

Scholz, C. H., Fractal transitions on geological surfaces, in *Fractals in th e Earth Sciences*, edited by C. C. Barton and P. LaPointe, pp. 131-140, Plenum, New York, 1995.

Shimazaki, K., Correlation between intraplate seismicity and interplate earthquakes in Tohoku, northeast Japan, *Bull. Seismol. Soc. Am.*, 68, 181-192, 1978.

Shimazaki, K., Small and large earthquakes: The effects of thickness of the seismogenic layer and the free surface, in *Earthquake Source Mechanics., Geophys. Monogr. Ser.*, vol. 37, edited by J. B. S. Das and C. Scholz, pp. 209-216, AGU, Washington, D.C., 1986.

Turcotte, D. L., Fractals in geology and geophysics, *Pure Appl. Geophys., 131*, 171-196, 1989.

Turcotte, D. L., *Fractals and Chaos in Geology and Geophysics*, 221 pp., Cambridge Univ. Press, NewYork, 1992.

Turcotte, D. L., *Fractals and Chaos in Geology and Geophysics*, 2nd. ed., 398 pp., Cambridge Univ. Press, New York,1997.

Usami, T., *Materials for Comprehensive List of Destructive Earthquakes in Japan*, Univ of Tokyo Press, Tokyo 1996.

Utsu, T., A method for determining the value of *b* in a formula $\log n = a - bM$ showing the magnitude frequency for earthquakes, *Geophys. Bull. Hokkaido Univ.,13*, 99-103,1965.

Utsu, T., Catalog of large earthquakes in the region of Japan from 1885 through 1980, *Bull. Earthquake. Res. Inst, Univ. Tokyo, 57*, 401-463,1982.

Xu, Y., and P. W. Burton, Spatial fractal evolutions and hierarchies for microearthquakes in central Greece, *Pure Appl. Geophys., 154*, 73-99, 1999.

Walsh, J. J., and J. Watterson, Fractal analysis of fracture patterns using the standard box-counting technique: Valid and invalid methodologies, *J. Struct. Geol., 15*, 1509-1512, 1993.

Warren, N.W., and G.V. Latham, An experimental study of thermally induced microfracturing and its relation to volcanic Seismicity, *J. Geophys. Res., 75*, 4455-4464, 1970.

Wesnousky, S. G., C. H.Scholz., K. Shimazaki and T. Matsuda, Integration of geological and seismological data for the analysis of seismic hazard: A case study of Japan, *Bull. Seismol. Soc. Am., 74*, 687-708, 1984.

Wilson, T. H., Non-fractal size-scaling attributes of fracture trace and Active fault networks with examples from the central Appalachians and Japan, *Geol. Soc. Am. Abstr. Programs, 31*,pp., A112, 1999.

Wilson, T. H., Size scaling relationships in fracture networks: Final research report of work conducted on D. O. E. contract DE-FG21-98FT40385, 89 pp, Natl. Energy Technol. Cent., Morgantown, W. Va., 2000.

Wilson, T. H., Size scaling relationships in fracture networks, *Math. Geol.*, 33, 591-613, 2001a.

Wilson, T. H., Scale transitions in fracture and active fault networks: *Math. Geol.,40p.*, in press, 2001b.

Wilson, T. H., J. Dominic, and J. Halverson, Fractal interrelationships in field and seismic data: Final research report of work conducted on D. O. E. contract DE-FG21-95MC32158, 162p, Natl. Energy Technol. Cent., Morgantown, W. Va., 1997.

O.Nishizawa, Geological Survey of Japan, 1-1-3 Higashi, Yatabe, Tsukuba-305-8567, Japan., (g0192@gsj.go.jp).

A.O.Öncel, Department of Geophysical Engineering, Engineering Faculty, Istanbul University, 34850-Avcılar-Istanbul/Turkey., (oncel@istanbul.edu.tr or oncel@hotmail.com)

T.H.Wilson, Department of Geology and Geography, West Wirginia University, 419 White Hall, Morgantown, WV 26506., (wilson@geo.wvu.edu)

(Received August 20, 1999; revised October 31, 2000; accepted November 7, 2000.)